AIP | Applied Physics Letters

The evolution of conducting filaments in forming-free resistive switching Pt/TaOx/Pt structures

F. Kurnia, Chunli Liu, C. U. Jung, and B. W. Lee

Citation: Applied Physics Letters **102**, 152902 (2013); doi: 10.1063/1.4802263
View online: http://dx.doi.org/10.1063/1.4802263
View Table of Contents: http://scitation.aip.org/content/aip/journal/apl/102/15?ver=pdfcov
Published by the AIP Publishing

The evolution of conducting filaments in forming-free resistive switching $Pt/TaO_x/Pt$ structures

F. Kurnia, Chunli Liu, C. U. Jung, and B. W. Lee[a)]
Department of Physics, Hankuk University of Foreign Studies, Yongin 449-791, South Korea

(Received 19 March 2013; accepted 5 April 2013; published online 16 April 2013)

The forming-free (FF) and forming-required (FR) resistive switching behaviors of $Pt/TaO_x/Pt$ structures were analyzed. Changes in the length and shape of the conducting filaments (CFs) suggested different evolution processes in the FF and FR cells when the CFs grew from weaker filaments to stronger ones. In the FR cells, the filament changed from a conical shape to a cylindrical shape with no change in length. In the FF cells, the filament maintained a cylindrical shape while increasing its diameter and decreasing its length. © *2013 AIP Publishing LLC* [http://dx.doi.org/10.1063/1.4802263]

Resistive switching (RS) phenomena have been studied in many oxide materials for their potential applications in nonvolatile resistive random access memory (RRAM) devices.[1] Binary oxides, such as NiO, TiO_2, and TaO_x, have attracted much interest because they can be prepared easily and are compatible with current complementary metal-oxide-semiconductor (CMOS) technology.[2–7]

Normal RS behavior consists of a SET process [from a high resistance state (HRS) to a low resistance state (LRS) at the set voltage V_S] and a RESET process (from the LRS to the HRS at the reset voltage V_R), each induced by an applied voltage. Switching between the HRS and LRS has been generally explained by the formation and rupture of metallic conducting filaments (CFs) in the oxide materials.[1–3] Most RRAM devices need a forming process to initiate the switching because the oxide materials/films used are initially insulating or highly resistive. During the forming process, the current flowing through the oxide film suddenly increases at the forming voltage (V_{FM}), which switches the device to the LRS. The value of V_{FM} is normally several times higher than V_S, leading to high power consumption and increased circuit and operational complexity. Therefore, developing an RRAM device with a lower V_{FM} or without the need for a forming process (i.e., forming-free switching) is desired.

Forming-free RS behaviors have been investigated by many recent reports. Fang *et al.*[8] used an $HfO_x/TiO_x/HfO_x/TiO_x$ multilayer to reduce V_{FM} near to V_S in a bipolar RS mode. Kim *et al.*[9] realized forming-free bipolar switching in $Pt/CuC/HfO_x/Pt$ structures with an ultrathin HfO_x layer. Additionally, forming-free unipolar RS behaviors have been reported in $Pt/TaO_x/Pt$ structures by this report's authors[7] and in $Al/Al_xO_y/Al$ structures by Zhu *et al.*[10] The forming-free RS behaviors presented in these reports are mainly due to the low-resistance initial state of the oxide films used, which can be attributed to metallic gradients such as metals or sub-oxides.

Although forming-free RS phenomena can also be explained by the formation and rupture of CFs, detailed switching characteristics have not yet been studied and compared with those of forming-required RS. In this study, we compare the two types of RS behaviors observed in $Pt/TaO_x/Pt$ structures: forming-required switching and forming-free switching. By analyzing their set voltages, reset currents, and resistances in the LRS, we show that the CFs in these two types of devices evolve differently when growing from weak to strong.

Amorphous TaO_x thin films were grown by pulsed laser deposition on $Pt/TiO_2/SiO_2/Si$ substrates at room temperature (25 °C) with an oxygen ambient pressure of 150 mTorr.[7,11] A KrF excimer laser with a wavelength of 248 nm was used to ablate a Ta_2O_5 ceramic target made from Ta_2O_5 powder. To fabricate the $Pt/TaO_x/Pt$ structures, ~100 nm Pt top electrodes were deposited on the TaO_x film by electron beam evaporation. The top electrode size was $90 \times 90\ \mu m^2$. Current-voltage (I-V) characteristics were measured using a semiconductor parameter analyzer (Agilent B1500A). During electrical characterization, the Pt bottom electrode was grounded, and a bias voltage was applied to the top electrode.

We observed unipolar resistive switching from almost all $Pt/TaO_x/Pt$ cells. Interestingly, depending on the position of the top electrode, each cell would exhibit one of two different switching behaviors [Fig. 1(a)]. One cell type started with low resistance, and resistive switching started with a RESET process, i.e., no forming process was necessary. Typical I-V curves are shown in Fig. 1(b). The other cell type started as an insulator; a forming process was required to induce resistive switching, as shown in Fig. 1(c). Hereafter we name the two types of cells as forming-free (FF) and forming-required (FR) cells, respectively.

We noticed that the FF and FR cells were not distributed randomly for one TaO_x film. Instead, they gathered at different locations on the TaO_x film, as shown in Fig. 1(a). Among the 20 cells made from one TaO_x film, about 75% of the cells showed FF switching (colored in gray), and the other 25% showed FR switching (colored in black). We confirmed this distribution by characterizing several TaO_x films grown at the same conditions. Therefore, the difference in switching behavior should be related to the properties of the TaO_x film at the different locations. Our previous study[7] showed that due to the existence of conductive Ta suboxides, the TaO_x film was conductive at the initial state, resulting in the forming-free switching behavior. The difference in the initial

[a)]Author to whom correspondence should be addressed. Electronic mail: bwlee@hufs.ac.kr

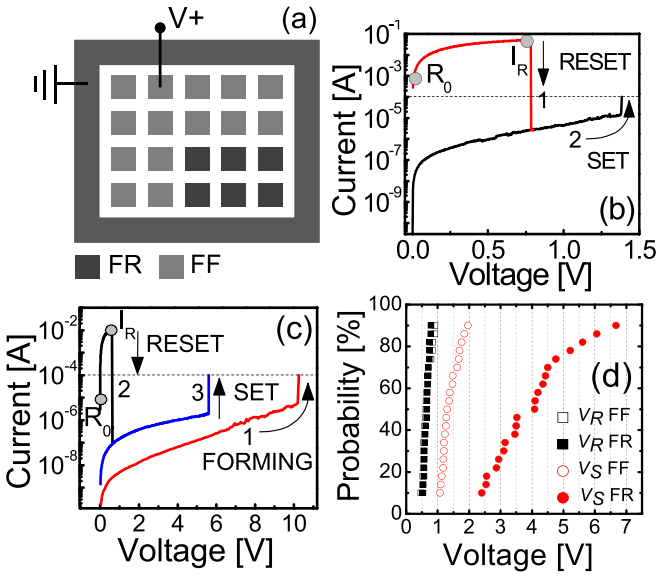

FIG. 1. (a) Measurement schematic of Pt/TaO_x/Pt devices and the distribution of FR and FF cells. (b) *I-V* characteristics of FF unipolar switching. (c) *I-V* characteristics of FR unipolar switching. (d) Cumulative probability of V_R and V_S in the FF and FR devices.

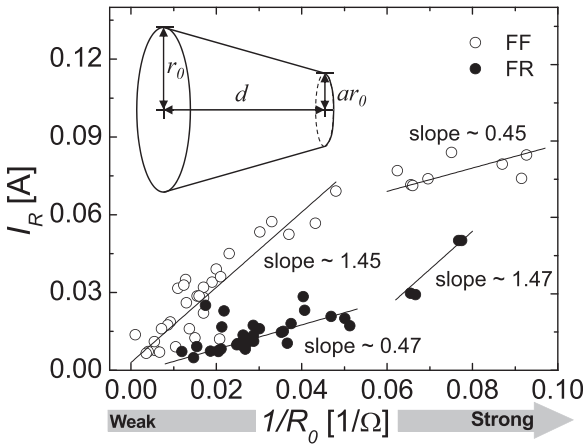

FIG. 2. The $I_R \sim 1/R_0$ relationship of the FF (open circle) and FR (filled circle) cells. The solid lines are eye guides to show changes of slope.

resistance of the FF and FR cells implies that the TaO_x film at the locations of the FF cells may have more Ta suboxides than that in the FR cells. This location dependence of the film properties could be caused by the relative position between the target (laser plume position) and the substrate.

In addition to having different forming characteristics, the two types of cells also had clearly different statistical distributions of V_S. Fig. 1(d) plots V_S and V_R of the FF and FR cells. Both types of cells had similar values of V_R (0.5–0.8 V) in narrow distributions. However, V_S varied significantly. The V_S of FF cells was 1.0–2.0 V, whereas for FR cells it had a much wider range of 2.5–7.0 V.

Because the unipolar RESET and SET processes can be explained by the formation and rupture of metallic CFs in the insulating oxide film, the difference in the forming process and the distribution of V_S for the two types of cells directly indicated that the CFs in each type have different evolution processes. As we reported in an earlier paper, the unipolar resistance switching in the Pt/TaO_x/Pt structure is originated from the redox reaction between Ta_2O_5 and Ta suboxides.[7] Because the TaO_x film is an n-type material with the O vacancies as the majority carriers, CFs were formed due to the migration of O vacancies and mainly consisted of Ta suboxides. Upon applying voltage bias, CFs form starting from the cathode and extending to the anode.[7,12] Therefore, it is reasonable to assume that a CF in this case has a conical shape with its radius decreasing from the cathode end to the anode end.

The shape and growth of conical CFs in a resistive switching cell with the forming process has been described using the relationship between the reset current I_R and the room temperature resistance of the CF R_0 (the resistance of the cell immediately after the SET process), as described by the following equation:

$$I_R \propto ad\left(\frac{1}{R_0}\right), \tag{1}$$

where a is the end-to-end diameter ratio of the CF between the anode and the cathode and d is the length of the CF, as shown in the inset of Fig. 2.[13] The CF is conical if $a \ll 1$ and is cylindrical if $a \sim 1$. Therefore, the slope of $I_R \sim 1/R_0$, which is proportional to the product ad, will give us information on the shape and length of the CF.

In Fig. 2 we plotted $I_R \sim 1/R_0$ for both types of cells. For the FR cells, I_R changes with $1/R_0$ following a similar trend to those reported for NiO and TiO_2 thin films,[13] where the slope of the $I_R \sim 1/R_0$ plot increases from a lower value at a high R_0 (weaker filament) to a higher value at a low R_0 (stronger filament). For FF cells, however, the slope changes in the opposite manner. Because the slope is determined by the product of a and d, additional characterization on these two parameters is necessary to clarify the change of a and d during the evolution process. Since d cannot be easily measured, we investigated the low resistance state of the CFs in both types of cells by measuring their resistances under the cathode and the anode. By comparing these resistances, we can get information about a.

Our measurement setup is similar to the one we used in a previous study.[7] However, instead of measuring the resistance in the HRS after the RESET process, we measured the resistance in the LRS after the SET process. As illustrated in Fig. 3(a), we switched the Pt/TaO_x/Pt/TaO_x/Pt structure using top electrodes 1 (anode) and 2 (cathode) and then measured the resistance of each Pt/TaO_x/Pt cell using either electrode 1 or 2 and the common Pt bottom electrode to get the resistances under the anode (R_A) and the cathode (R_C), respectively.[7,12] The FR cells were measured using a similar procedure. In this case, the total resistance of the CF for the Pt/TaO_x/Pt/TaO_x/Pt structure is the sum of R_A and R_C, which will be called R_{CF}. Note that this parameter corresponds to R_0 in Fig. 2 for the simple Pt/TaO_x/Pt structure.

Figs. 3(a)–3(c) reveal different relationships between R_A, R_C, and R_{CF} for the two types of cells. For the FR cell, when the filament is weaker (larger R_{CF}), R_A is about 4 times greater than R_C [Figs. 3(b) and 3(d)]. When the filament grows stronger (smaller R_{CF}), R_A decreases quickly while R_C barely changes. We can understand this process by the following mechanism: The filament starts with a conical shape that has a wider end under the cathode and a much narrower

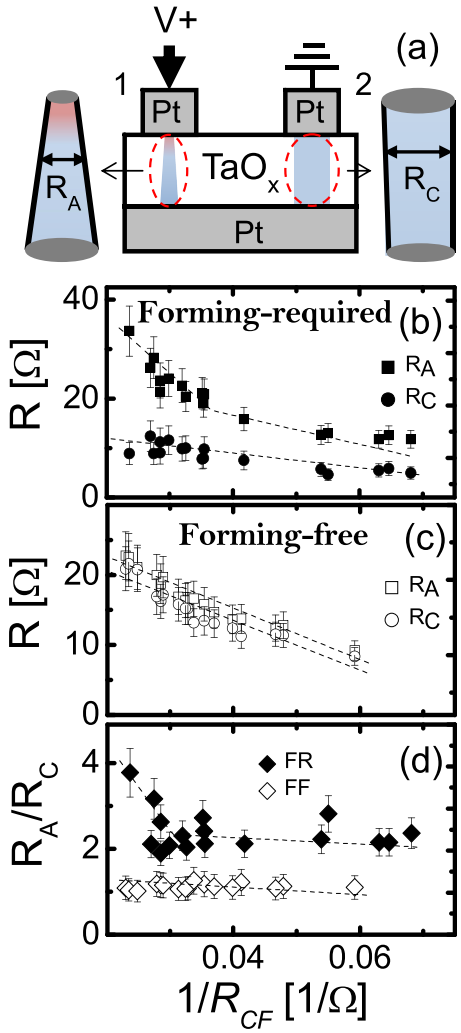

FIG. 3. (a) Top-to-top configuration schematic for a Pt/TaO$_x$/Pt/TaO$_x$/Pt device. Changes of R_A and R_C vs. the total resistance of the CF in LRS are plotted in (b) for the FR cell and in (c) for the FF cell. (d) The anode-to-cathode resistance ratio R_A/R_C calculated from (b) and (c). The dashed lines are guides for the eyes.

end under the anode. During filament growth, the anode end expands more quickly; as a result, the filament becomes more cylindrical with a reduced resistance. Therefore, a should change from $a \ll 1$ to $a \sim 1$.

For FF cells, though, R_A and R_C always have very similar values that change at the same rate [Fig. 3(c)]. This behavior means that the filament has the same diameter at both ends, and the two ends expand simultaneously. The filament may start with a narrower cylindrical shape and then grow wider with a reduced resistance. In this case, a should have a constant value close to 1.

Based on the information obtained for a from Figs. 2 and 3, we can obtain information about the length of CFs for the two types of cells. Considering the constant value of $a \approx 1$ revealed from Figs. 3(c) and 3(d), the slope change for the $I_R \sim 1/R_0$ plot of FF cells in Fig. 2 implies that the length d of a weak CF is much longer than that of a stronger one. For the FR cells, during the forming process the large forming voltage and compliance current will form a path connecting the two electrodes, preferentially along the shortest path. Thus, the initial effective length of the filament is already equal or close to the thickness of the film and does not change much thereafter.[3,13] Therefore, the slope change in Fig. 2 for the FR cells is mainly due to the increase in a, which implies that the filament grows from a conical shape to a more cylindrical shape.

This analysis indicates that the CFs in the FF cells evolve quite differently than those in the FR cells. The schematic plots in Figs. 4(a)–4(c) illustrate the development process of CFs in the FF cells. The initial conducting state of the as-deposited TaO$_x$ film implies that there are many pre-existing filaments. These filaments could have formed because of the presence of Ta suboxides, which are more conductive than Ta$_2$O$_5$.[7] These pre-existing filaments should be distributed randomly in the film, meaning the CFs may form zig-zag shapes [Fig. 4(a)] instead of connecting the cathode and anode along a straight line. When voltage is first applied, current will flow along these filaments, and the total length connecting the anode and cathode should be much longer than the film thickness [Fig. 4(a)]. When the applied voltage increases, more pre-existing filaments become connected and the CFs expand [Fig. 4(b)]. Finally, when enough pre-existing filaments connect together, the CFs act like straight paths connecting the anode and the cathode, decreasing the length d to be equal to the film thickness [Fig. 4(c)]. R_A and R_C increase by about a multiple of 3 (from $\sim$9 Ω to $\sim$25 Ω) in Fig. 3(b), agreeing well with the decrease of d ($\sim$3 times) considering the slope change in Fig. 2.

The CF development process for a FR cell is illustrated in Figs. 4(d)–4(f). After the forming process, a nearly straight path connecting the two electrodes is formed. The anode end is narrower due to the Ta$_2$O$_5$ being n-type;[7,12,14] thus, R_A is larger than R_C. This resistance difference is more

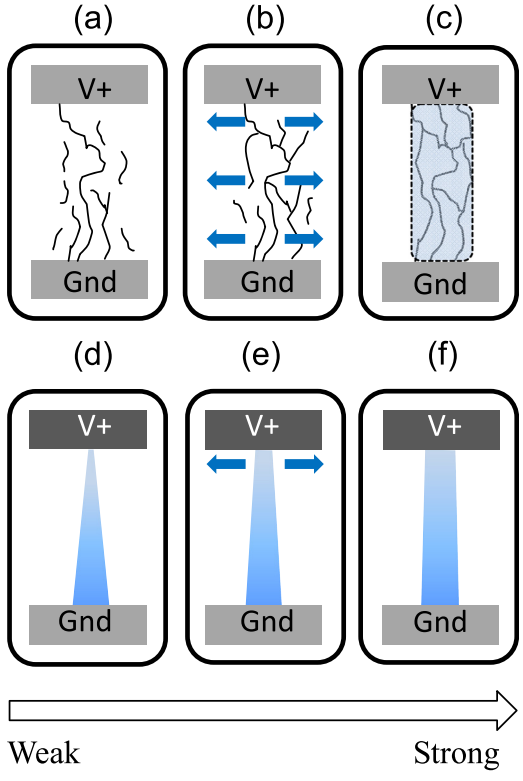

FIG. 4. Schematic illustration of the evolution process of CFs in (a)–(c) FF and (d)–(f) FR cells.

significant when the filament first forms and is weak [Fig. 4(d)], as indicated by the ratio of R_A/R_C in Figs. 3(b) and 3(d). During the evolution process, the expansion of the filament under the anode will dominate the growth of the CF, causing its shape to become more cylindrical. The relationship between the changes in a and the R_A/R_C ratio in the FR cells can be quantitatively correlated considering the conical shape of the CF. Since R_A is larger than R_C and the CF ruptures under the anode, the conical geometry should be used to calculate R_A. On the other hand, since R_C is always in an LRS[7] and does not change much during its evolution [Fig. 3(b)], the cylindrical shape can be assumed to calculate R_C as illustrated in Fig. 3(a). If we take the radius of R_C as r_0, the cathode and anode radius of R_A as r_0 and ar_0, respectively, and the length of both R_A and R_C as l (≈film thickness), R_A and R_C can be expressed using the following equations:[15]

$$R_A = \left(\frac{\rho}{2\pi a}\right)\frac{(1-a)^2}{\sqrt{l^2 + r_0^2(1-a)^2} - l}, \tag{2}$$

$$R_C = \rho\frac{l}{\pi r_0^2}. \tag{3}$$

Considering that the length of the filament is usually much greater than its radius, i.e., $l/r_0 \gg 1$, a can be simply expressed as $a \geq R_C/R_A$. In Fig. 3(d), R_A/R_C changes at most from about 1.8 to 4.6 (about 2.5 times) when a weaker CF grows to a stronger one; therefore, the change in a should be a little bit larger than 2.5. In Fig. 2, a increases about 3 times during filament growth as estimated from the slope and therefore agrees reasonably well with the data shown in Figs. 3(b) and 3(d).

This analysis also helps us understand the connection between the forming process and the switching parameters. Due to the many pre-existing filamentary paths in the pristine devices, CFs can easily re-connect along similar paths after rupture, meaning V_S does not change much. However, for the FR devices the insulating nature of the oxide film requires higher and randomly distributed V_S values to reconnect the CFs.[3] Since reducing the widely distributed V_S range is one of the most challenging tasks in RRAM research, the forming-free characteristics and narrow distribution of V_S from the initial conductivity of the oxide film are advantageous for practical applications of RRAM devices. We also noticed that the reset currents of the FF cells are higher than the FR cells due to the stronger filament under the anode in the FF cells as shown in Figs. 3 and 4. Reducing the size of the electrode or adjusting the film composition could provide possible solutions for reducing the reset current in the FF cells.

In summary, we analyzed and compared the evolution processes of CFs in Pt/TaO_x/Pt structures with FF and FR unipolar resistance switching types. During evolution from weaker filaments to stronger ones, the growth of conical CFs in FR devices was dominated by lateral expansion at the anode end. For FF devices, the cylindrical CFs within shortened and laterally expanded at both ends equally. Our results indicate that by carefully adjusting the composition of the TaO_x thin film, it is possible to prepare forming-free unipolar RS devices with uniform set voltages.

This research was supported by the Basic Science Research Program through the National Research Foundation of Korea (NRF) funded by the Ministry of Education, Science and Technology (2012R1A1A2008595, 2012R1A1A2008845, and 2012R1A1A3009736).

[1]R. Waser, R. Dittmann, G. Staikov, and K. Szot, Adv. Mater. **21**, 2632 (2009).
[2]D.-H. Kwon, K. M. Kim, J. H. Jang, J. M. Jeon, M. H. Lee, G. H. Kim, X.-S. Li, G.-S. Park, B. Lee, S. Han, M. Kim, and C. S. Hwang, Nat. Nanotechnol. **5**, 148 (2010).
[3]S. C. Chae, J. S. Lee, S. Kim, S. B. Lee, S. H. Chang, C. Liu, B. Kahng, H. Shin, D.-W. Kim, C. U. Jung, S. Seo, M.-J. Lee, and T. W. Noh, Adv. Mater. **20**, 1154 (2008).
[4]K. M. Kim, D. S. Jeong, and C. S. Hwang, Nanotechnology **22**, 254002 (2011).
[5]M.-J. Lee, S. Han, S. H. Jeon, B. H. Park, B. S. Kang, S.-E. Ahn, K. H. Kim, C. B. Lee, C. J. Kim, I.-K. Yoo, D. H. Seo, X.-S. Li, J.-B. Park, J.-H. Lee, and Y. Park, Nano Lett. **9**, 1476 (2009).
[6]K. Kinoshita, T. Tamura, M. Aoki, Y. Sugiyama, and H. Tanaka, Appl. Phys. Lett. **89**, 103509 (2006).
[7]F. Kurnia, H. Hadiyawarman, C. U. Jung, R. Jung, and C. Liu, Phys. Status Solidi (RRL) **5**, 253 (2011).
[8]Z. Fang, H. Y. Yu, X. Li, N. Singh, G. Q. Lo, and D. L. Kwong, IEEE Electron Device Lett. **32**, 566 (2011).
[9]S. Kim, M. Jo, J. Park, J. Lee, W. Lee, and H. Hwang, Electrochem. Solid-State Lett. **14**, H322 (2011).
[10]W. Zhu, T. P. Chen, Z. Liu, M. Yang, Y. Liu, and S. Fung, J. Appl. Phys. **106**, 093706 (2009).
[11]B. W. Lee and C. U. Jung, Appl. Phys. Lett. **96**, 102507 (2010).
[12]K. M. Kim, B. J. Choi, Y. Ch. Shin, S. Choi, and C. S. Hwang, Appl. Phys. Lett. **91**, 012907 (2007).
[13]K. M. Kim, M. H. Lee, G. H. Kim, S. J. Song, J. Y. Seok, J. H. Yoon, and C. S. Hwang, Appl. Phys. Lett. **97**, 162912 (2010).
[14]K. M. Kim and C. S. Hwang, Appl. Phys. Lett. **94**, 122109 (2009).
[15]D. J. Griffiths, *Introduction to Electrodynamics* (Prentice-Hall, New Jersey, 1999), p. 334.